Self-assembly of amorphous biophotonic nanostructures by phase separation†

Eric R. Dufresne,*[ab] Heeso Noh,[ab] Vinodkumar Saranathan,[c] Simon G. J. Mochrie,[ab] Hui Cao[ab] and Richard O. Prum*[c]

Received 11th February 2009, Accepted 11th March 2009
First published as an Advance Article on the web 30th March 2009
DOI: 10.1039/b902775k

Some of the most vivid colors in the animal kingdom are created not by pigments, but by wavelength-selective scattering of light from nanostructures. Here we investigate quasi-ordered nanostructures of avian feather barbs which produce vivid non-iridescent colors. These β-keratin and air nanostructures are found in two basic morphologies: tortuous channels and amorphous packings of spheres. Each class of nanostructure is isotropic and has a pronounced characteristic length scale of variation in composition. These local structural correlations lead to strong backscattering over a narrow range of optical frequencies and little variation with angle of incidence. Such optical properties play important roles in social and sexual communication. To be effective, birds need to precisely control the development of these nanoscale structures, yet little is known about how they grow. We hypothesize that multiple lineages of birds have convergently evolved to exploit phase separation and kinetic arrest to self-assemble spongy color-producing nanostructures in feather barbs. Observed avian nanostructures are strikingly similar to those self-assembled during the phase separation of fluid mixtures; the channel and sphere morphologies are characteristic of phase separation by spinodal decomposition and nucleation and growth, respectively. These unstable structures are locked-in by the kinetic arrest of the β-keratin matrix, likely through the entanglement or cross-linking of supermolecular β-keratin fibers. Using the power of self-assembly, birds can robustly realize a diverse range of nanoscopic morphologies with relatively small physical and chemical changes during feather development.

In contrast to pigmentary colors, structural colors are produced by optical interactions with nanoscale variations in refractive index.[1,2] Organismal structural colors can be produced by photonic crystals.[2] In addition to these highly periodic structures, biological photonic nanostructures also include amorphous, or quasi-ordered, dielectric nanostructures where there are local correlations but little long-range order.[3]

An important fundamental question for understanding the function and evolution of structural coloration of organisms is how these nanostructures develop during individual growth. Variations in the dimensions of a nanostructure will produce visible variations in color that may result in ineffective social or sexual communication signals. Thus, nanostructure development must be precisely controlled to produce appropriate color phenotypes. Inside the body of butterfly scales, color-producing air–chitin nanostructures develop from a biological template produced by complex growth of the cellular

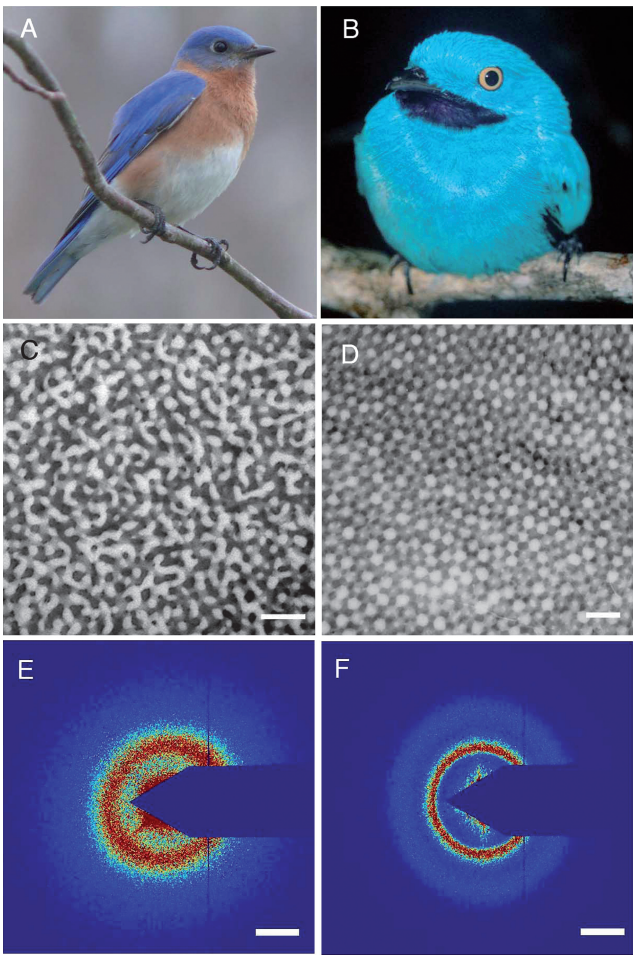

Fig. 1 (A) Male Eastern Bluebird (*Sialia sialis*, Turdidae). (B) Male Plum-throated Cotinga (*Cotinga maynana*, Cotingidae). (C) Channel-type β-keratin and air nanostructure from back contour feather barbs of *S. sialis*. (D) Sphere-type β-keratin and air nanostructure from back contour feather barbs of *C. maynana*. (E) Small-angle X-ray scattering data from channel-type feather barb of *S. sialis*.. (F) Small-angle X-ray scattering data from sphere-type feather barb of *C. maynana*. Scale bars (C–D) 500 nm, (E–F) 0.025 nm^{-1} of spatial frequency. Photo credits: (B) Ken Thomas (image in the public domain); (B) Thomas Valqui (reproduced with permission).

[a]*School of Engineering and Applied Science, Yale University, New Haven, CT, 06511, USA. E-mail: eric.dufresne@yale.edu*
[b]*Department of Physics, Yale University, New Haven, CT, 06511, USA*
[c]*Department of Ecology and Evolutionary Biology, Peabody Museum of Natural History, Yale University, New Haven, CT, 06511, USA. E-mail: richard.prum@yale.edu*

† Electronic supplementary information (ESI) available: Supplementary methods and figure captions; Fig. S1–S3. See DOI: 10.1039/b902775k

membrane and smooth endoplasmic reticulum.[4] In contrast, biophotonic crystals can develop by colloidal self-assembly in iridescent macrospores of *Sellaginella*.[5] Here, we consider the hypothesis that the photonic nanostructures in avian feather barbs self-assemble as β-keratin phase separates from cytoplasm within medullary cells.

Structural colors of avian feather barbs are produced by light scattering from spongy β-keratin and air nanostructures within the medullary cells of avian feather barb rami.[6,7] Feathers are composed almost entirely of feather β-keratins, which are β-pleated-sheet proteins that self-assemble into filaments.[8,9] Two distinct classes of quasi-ordered, 3D nanostructures have been recognized.[7,10] Channel-type nanostructures have β-keratin bars and air channels in tortuous and twisting forms. The channel morphology is found in the blue back plumage of the Eastern Bluebird (*Sialia sialis*) (Fig. 1A,C). Spherical nanostructures consist of nearly close-packed spherical air cavities, sometimes with small interconnections. The sphere morphology is found in the vivid turquoise-blue plumage of the Plum-throated Cotinga (*Cotinga maynana*) (Fig. 1B,D). A phylogenetic survey of avian structural colors indicates that channel and sphere nanostructures have evolved independently in many lineages of birds.[7]

Amorphous β-keratin nanostructures have interesting optical properties that are used by birds in social signaling.[7] Here, we describe the optical properties of bird feathers by measuring the reflectance as a function of wavelength, incident angle and exit angle (see ESI, Fig. S1†).

In both *Sialia sialis* and *Cotinga maynana*, scattering is the strongest in the backward direction (Fig. S2), so we report only the backscattering data here. The spectra of backscattered light are peaked in both species (Figs. 2A–B). The channel nanostructure of *S. sialis* produces a substantially broader reflectance peak (Fig. 2A) than does the spherical nanostructure of *C. maynana* (Fig. 2B). The intensity and position of the peaks in backscattered light are relatively constant over incident angles from normal (5°) to 65°. The backscattering intensity drops rapidly at higher angles of incidence.

The optical properties of these nanostructures are determined by their structure. We use small-angle X-ray scattering (SAXS) to quantify the 3D structure *in situ* of the channel- and sphere-type nanostructures of *S. sialis* and *C. maynana*, respectively. SAXS directly measures the structural correlations that lead to the scattering of light, without complications due to multiple scattering. The X-ray scattering spectra of both the channel and sphere nanostructures are isotropic (Fig. 1E–F). Exploiting this symmetry, we average the scattering intensity over azimuthal angles. We observe a strong peak in the scattering intensity as function of spatial frequency, q, for both species (Fig. 2C–D). This indicates a dominant length scale for structural correlations, leading to peaks in the scattering intensity at 0.036 and 0.030 nm^{-1} for *S. sialis* and *C. maynana*, respectively. The two scattering profiles are distinguished by a noticeable difference in the widths of their principle scattering peaks with channel-type *S. sialis* showing a wider peak: (peak width)/(peak position) = 0.45 and 0.16 for *S. sialis* and *C. maynana*, respectively. In addition, a second weaker peak occurs at higher spatial frequency for the spherical *C. maynana* nanostructure (Fig. 2D), but not for *S. sialis*.

We can directly compare the optical measurements and X-ray scattering data by plotting both scattered intensity and the back-reflected spectrum as a function of the scattered wavevector $q = (4\pi n_{av}\cos\theta/2)/\lambda$ (Fig. 2C–D). The positions of the peaks in the

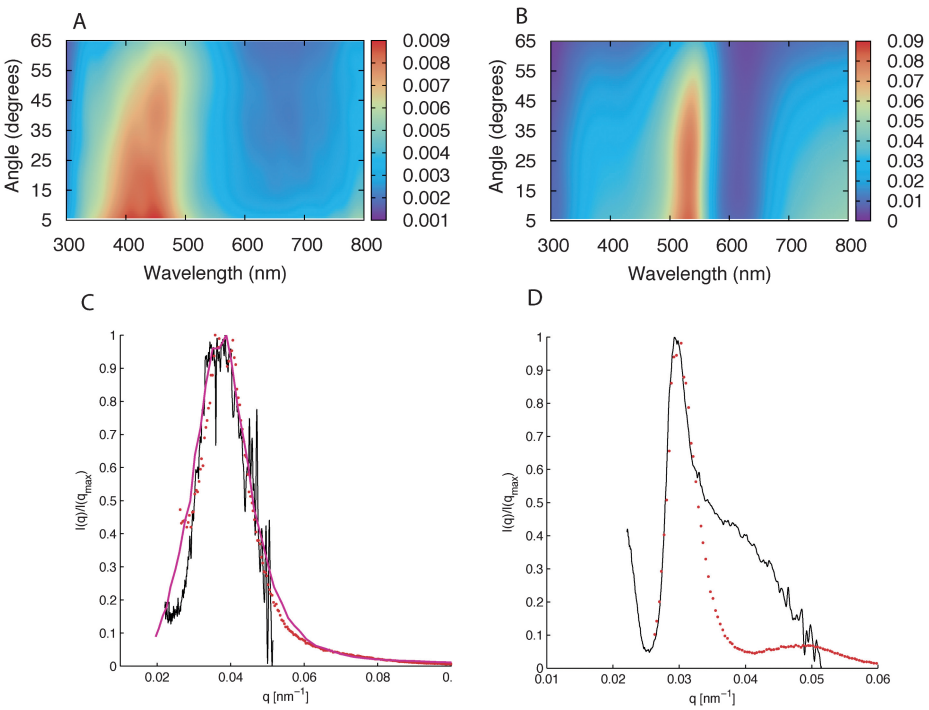

Fig. 2 (A–B) Back-scattered intensity for incident angles from normal (5°) to 65° for (A) Eastern Bluebird *Sialia sialis* and (B) Plum-throated Cotinga (*Cotinga maynana*). (C–D) Azimuthal averages of small angle X-ray scattering data (red dots) in comparison to backscatttered intensity at normal incidence (black lines) plotted as a function of q (spatial frequency in nm^{-1}) for (C) *S. sialis* and (D) *C. maynana*. The scattering intensity of the channel-type nanostructure of *S. sialis* (C) is also compared to light scattering data collected from a polymer mixture undergoing phase separation by spinodal decomposition[15] (red line, C). All data are normalized to the maximum intensity, $I(q_{max})$.

scattered intensity agree nicely for both species using an average refractive index of 1.25, which is similar to previous estimates based on electron micrographs.[6,7] The index of refraction of β-keratin is reported to be 1.58,[11] which suggests that the volume fraction of air in the nanostructures is 0.62. There is excellent agreement between the optical and X-ray spectra over the entire range of sampled q for *S. sialis*. This shows that scattering from *S. sialis* is relatively weak – *i.e.* all of the backscattered light has been scattered only once by the feather nanostructure. On the other hand, there is significant disagreement in the shape of the optical and X-ray spectra for *C. maynana*, suggesting that scattering from this sample is strong – *i.e.* each photon has a much higher probability of being scattered by the nanostructure, resulting in a significant contribution of multiply scattered photons to the backscattering signal. Indeed, the reflectance peak of *C. maynana* is about eight times brighter than that of *S. sialis*.

To guarantee robust communication function, birds must be able to precisely control nanostructure formation during feather development. TEM observations of blue feather barbs of Blue-and-yellow Macaw (*Ara ararauna*) indicate that the nanostructures are self-assembled without biological prepattern of cellular membranes or intermediate filaments.[12] The β-keratin/air nanostructures found in feather barbs are strikingly similar to morphologies observed in the phase separation of polymers in a solvent.[12,13] While entropy favors mixing, repulsions between dissimilar molecules favor macroscopic phase separation, like oil and water. For a given temperature and composition, thermodynamics determines whether the system will be mixed or phase-separated. In the phase diagram (Fig. 3, top), states above the phase boundary, like point A, remain mixed, while states below the phase boundary, like B and C, separate into two macroscopic phases with distinct compositions. As thermodynamic parameters – composition, interaction strength, and temperature – change over time, a mixed system can be driven to phase separate, or "unmix". Phase separation occurs through two possible morphological pathways: spinodal decomposition (SD) or nucleation and growth (N&G). The position in phase space relative to the spinodal line (dashed line, Fig. 3, top) determines which pathway is selected. If the mixture lies between the phase boundary and the spinodal line, as in B (Fig. 3, top), then phase separation occurs through a process of nucleation and growth, which is characterized by the formation of isolated spherical droplets of the minority phase. If nucleation is fast and growth is relatively slow, highly monodisperse (*i.e.* identically sized) droplets are formed. When the unmixed state lies below the spinodal line, as in C (Fig. 3, top), then phase separation proceeds by a process called spinodal decomposition, where the system forms channel-like structures that increase their compositional contrast and coarsen over time.[13]

We hypothesize that the photonic nanostructures in avian feathers are self-assembled by the phase separation of β-keratin from the cellular cytoplasm. In feathers, we expect that polymerization of β-keratin drives phase separation. β-Keratin polymerizes to form long supermolecular filaments under the normal physiological conditions within a cell.[8] As the molecular weight of the filaments increases, the entropic incentive to mixing drops and the phase boundary shifts to higher temperatures (Fig. 3, bottom). As the position of the phase boundaries shift over time, phase separation by either SD or N&G could proceed without changes in composition (Fig. 3, bottom).

While thermodynamics favors complete macroscopic phase separation into two distinct compositions, phase separation can be

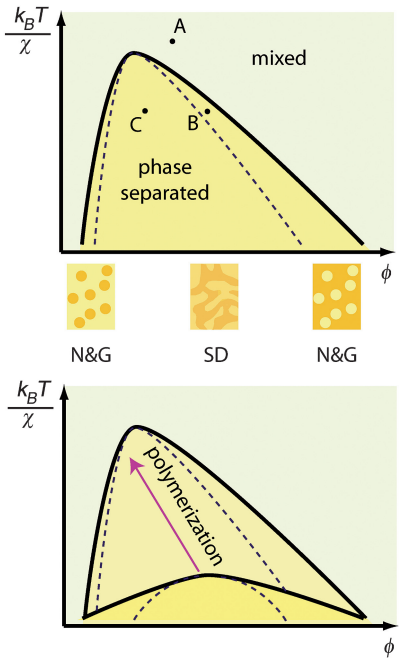

Fig. 3 (Top) Schematic phase diagram of a polymer solution, as a function of polymer volume fraction, ϕ, temperature, T, and interaction parameter, χ. Above the phase boundary (black line) at A, the system is a one-phase mixture. Below, the phase boundary, the solution separates into two distinct phases. Below the spinodal line (dashed line) at C, phase separation happens *via* spinodal decomposition (SD) forming a tortuous network of the two phases. Between the spinodal line and the phase boundary at B, phase separation occurs through the isolated nucleation and growth (N&G) of spherical droplets of the minority phase. Schematics of the characteristic structures produced in each region of phase separation are shown along the ϕ axis. (Bottom) As polymerization proceeds (arrow), the position of the phase boundary and the spinodal line changes. Thus, stable compositions can be driven to phase separate by polymerization.

arrested at an intermediate state by the vitrification or gelation of one of the two phases. For example, arrested spinodal decomposition has recently been observed in deep-quenched solutions of a globular protein, lysozyme.[14] In feathers, arrest of phase separation would be facilitated by the entanglement or crosslinking of long β-keratin filaments. In this model, birds develop color producing nanostructures by controlling the combined process of phase separation and kinetic arrest with three variables: the rates of β-keratin expression, β-keratin polymerization, and filament crosslinking.

As a preliminary test of the phase separation hypothesis, we compare the X-ray scattering intensities from *S. sialis* to light scattering data collected from a polymer mixture (polybutadiene and polyisoprene) undergoing phase separation by spinodal decomposition[15] (Fig. 2C). The azimuthal average of the SAXS data from the channel nanostructure of *S. sialis* shows excellent correspondence to the spinodal data (red line, Fig. 2C) The spherical nanostructures of *C. maynana* show a distinct, higher spatial frequency peak that reflects the short-range structural correlations in the close packing of relatively monodisperse spheres (Fig. 2D), as could be expected from phase separation with rapid nucleation, and slow growth.

Structural measurements support the conclusion that the nanostructures of color-producing spongy feather β-keratins are

self-assembled during phase separation of β-keratin from other cytoplasmic components. Channel-type nanostructures conform quantitatively to structures formed by spinodal decomposition. Sphere nanostructures appear in qualitative agreement with the more variable nucleation-and-growth mechanism. The phase separation hypothesis explains the distinctive and stereotyped shapes of color-producing β-keratin feather nanostructures.[7,10] The phase separation hypothesis may also provide new insights into the multiple evolutionary origins of both channel- and sphere-type nanostructures within birds.

More research is needed to elucidate the cellular mechanisms regulating the phase separation and kinetic arrest of β-keratin within the medullary cells. Biomimetic phase separation may provide a novel route for the assembly of useful photonic nanostructures.[16]

Acknowledgements

This work was supported with seed funding from the Yale NSF-MRSEC (DMR-0520495) and NSF grants to ERD (CBET), SGJM (DMR), HC (EECS), and ROP (DBI). Feather specimens were provided by the Yale Peabody Museum of Natural History and the University of Kansas Natural History Museum and Biodiversity Research Center. TEMs of feathers were prepared by Tim Quinn. SAXS data were collected at beam line 8-ID-I at the Advanced Photon Source at Argonne National Labs with the help of Drs. Alec Sandy and Suresh Narayanan, and supported by the U. S. Department of Energy, Office of Science, Office of Basic Energy Sciences, under Contract No. DE-AC02-06CH11357.

Notes and references

1 M. Srinivasarao, *Chemical Reviews*, 1999, **99**, 1935–1961.
2 P. Vukusic and J. R. Sambles, *Nature*, 2003, **424**, 852–855.
3 R. O. Prum and R. H. Torres, *Integrative and Comparative Biology*, 2003, **43**, 591–602.
4 H. Ghiradella, *J. Morph.*, 1989, **202**, 69–88.
5 A. R. Hemsley, M. E. Collinson, W. L. Kovach, B. Vincent and T. Williams, *Phil. Trans. R. Soc. Lond.*, 1994, **345**, 163–173; A. R. Hemsley, P. D. Jenkins, M. E. Collinson and B. Vincent, *Botanical Journal of the Linnean Society*, 1996, **121**, 177–187.
6 R. O. Prum, R. H. Torres, S. Williamson and J. Dyck, *Nature*, 1998, **396**, 28–29; R. O. Prum, R. H. Torres, S. Williamson and J. Dyck, *Proceedings of the Royal Society London B*, 1999, **266**, 13–22.
7 R. O. Prum, in *Bird Coloration, Volume 1 Mechanisms and Measurements*, edited by G. E. Hill and K. J. McGraw (Harvard University Press, Cambridge, MA, 2006), Vol. 1, pp. 295–353.
8 A. H. Brush, *Journal of Protein Chemistry*, 1983, **2**, 63–75.
9 A. H. Brush, in *Chemical Zoology*, edited by A. H. Brush (Academic Press, New York, 1978), Vol. 10, pp. 141–164.
10 J. Dyck, *Proc. Int. Ornithol. Congr.*, 1976, **16**, 426–437s.
11 D. J. Brink and N. G. van der Berg, *Journal of Physics D: Applied Physics*, 2004, **37**, 813–818.
12 R. O. Prum, E. R. Dufresne, T. Quinn and K. Waters, *Journal of the Royal Society Interface*, 2009, **6**, S253–S265.
13 R. A. L. Jones, *Soft Condensed Matter* (Oxford University Press, Oxford, U.K., 2002).
14 F. Cardinaux, T. Gibaud, A. Stradner and P. Schurtenberger, *Phys. Rev. Lett.*, 2007, **99**, 118301.
15 M. Takenaka and T. Hashimoto, *Journal of Chemical Physics*, 1992, **96**, 6177–6190.
16 A. R. Parker and H. E. Townley, *Nature Nanotechnology*, 2007, **2**, 347–353.